Available online at www.sciencedirect.com
ScienceDirect
Geomorphology 90 (2007) 283–301
GEOMORPHOLOGY
www.elsevier.com/locate/geomorph

Embedding reach-scale fluvial dynamics within the CAESAR cellular automaton landscape evolution model

Marco J. Van De Wiel [a,*], Tom J. Coulthard [b], Mark G. Macklin [c], John Lewin [c]

[a] Department of Geography, University of Western Ontario, London, Ontario, Canada
[b] Department of Geography, University of Hull, Hull, UK
[c] Institute of Geography and Earth Sciences, University of Wales, Aberystwyth, UK

Accepted 16 October 2006
Available online 21 April 2007

Abstract

We introduce a new computational model designed to simulate and investigate reach-scale alluvial dynamics within a landscape evolution model. The model is based on the cellular automaton concept, whereby the continued iteration of a series of local process 'rules' governs the behaviour of the entire system. The model is a modified version of the CAESAR landscape evolution model, which applies a suite of physically based rules to simulate the entrainment, transport and deposition of sediments. The CAESAR model has been altered to improve the representation of hydraulic and geomorphic processes in an alluvial environment. In-channel and overbank flow, sediment entrainment and deposition, suspended load and bed load transport, lateral erosion and bank failure have all been represented as local cellular automaton rules. Although these rules are relatively simple and straightforward, their combined and repeatedly iterated effect is such that complex, non-linear geomorphological response can be simulated within the model. Examples of such larger-scale, emergent responses include channel incision and aggradation, terrace formation, channel migration and river meandering, formation of meander cutoffs, and transitions between braided and single-thread channel patterns. In the current study, the model is illustrated on a reach of the River Teifi, near Lampeter, Wales, UK.

Keywords: Alluvial geomorphology; Landscape evolution; Cellular automaton; Simulation; River Teifi

1. Introduction

Most of the immediately recognizable elements of the alluvial landscape (*e.g.* channel patterns, terraces, meander cut-offs, levees) develop over time scales of decades to centuries. Yet their development and evolution results from the interactions between a range of geomorphological processes that typically operate over much smaller spatial and temporal scales (*e.g.* sediment entrainment and transport, river bank failure, overbank deposition).

Applying the same reductionist concept to the numerical modelling of alluvial landscape evolution requires representation of the geomorphic processes at sufficiently fine spatial and temporal resolution. Over the last decades different computational techniques have been developed that lend themselves to such high-resolution process representation, most notably the application of 2D and 3D computational fluid dynamics (CFD) in geomorphological studies (*e.g.* Bates and Lane, 2000). However, these studies tend to focus on

* Corresponding author.
E-mail address: mvandew3@uwo.ca (M.J. Van De Wiel).

0169-555X/$ - see front matter © 2007 Elsevier B.V. All rights reserved.
doi:10.1016/j.geomorph.2006.10.024

small-scale and short-term investigations, because CFD modelling is currently too computationally demanding to be applied to catchment evolution over time scales of decades or centuries. Such large-scale simulations are generally performed using cellular automaton landscape evolution models or alluvial architecture models (Coulthard, 2001; Willgoose, 2005; Coulthard et al., 2007-this issue). However, most of these models operate on a relatively coarse resolution (*i.e.* 50 m to 500 m spatially; and 1 day to 1+ years temporally). At these resolutions the small-scale geomorphic processes are represented either as probabilistic events in space and time (*e.g.* avulsion), or through some sort of statistically averaged effect (*e.g.* sediment entrainment).

In this paper we present a numerical model, which aims to address these issues through computationally efficient high-resolution simulation of alluvial landscape evolution. The model is a development of the CAESAR model (Coulthard et al., 2000, 2002, 2005), and includes new or enhanced routines for flow routing, sediment transport, sediment suspension and lateral erosion. These new routines allow simulation of point bar formation, floodplain deposition (splays and levees), river bank erosion, channel migration, and terrace formation. The model can operate on a range of spatial resolutions. This permits application of the same model in different settings, notably a high-resolution mode for alluvial river reaches, and a coarser-resolution mode for the upstream and tributary catchments.

2. Computational techniques

2.1. Model structure

The model presented herein is a development of the CAESAR landscape evolution model (Coulthard et al., 2000, 2002, 2005). It is based on the cellular automaton (CA) concept, whereby the continued iteration of a series of local process 'rules' governs the behaviour of the entire system. Although these rules are relatively simple and straightforward representations of fluvial and hillslope processes, their combined and repeatedly iterated effect is such that complex non-linear geomorphological response can be simulated within the model. Both positive and negative feedbacks between form and process can emerge.

CAESAR can be run in two modes: a catchment mode, with no external influxes other than rainfall; and a reach mode, with one or more points where sediment and water enter the system. In both modes the model requires the specification of various spatially distributed landscape parameters (initial conditions): elevation, roughness, grain sizes and vegetation cover. These spatial distributions are represented on a grid of cells, the resolution of which is specified through a cell spacing or cell width, c_w. The temporal input requirements (forcing conditions) vary according to the mode in which the simulation is run. In catchment mode, the model requires rainfall data for the duration of the simulation; in reach mode, it requires discharges and sediment fluxes for all inflow points. These temporal data are usually specified at hourly intervals.

Landscape simulation in CAESAR follows a simple structure (Fig. 1), whereby topography drives fluvial and hillslope processes that determine the spatial distribution of erosion and deposition for a given time step. This alters the topography, which becomes the starting point for the next time step. The model uses variable length time steps, depending on the rates of erosion and deposition occurring within the system (see below). Outputs of the model are elevation and sediment distributions through space and time, and discharges and sediment fluxes at the outlet(s) through time. Additional fluxes at specified points in the catchment or reach can be easily obtained.

2.2. Flow routing

Flow is the main driver for the geomorphological processes in alluvial environments. Although highly accurate solutions for flow depth and flow velocity can be obtained from traditional computational fluid dynamic approaches, such as finite difference solutions to either full or depth-averaged Navier–Stokes equations (Lane, 1998), these techniques are computationally too demanding to be used in landscape evolution models. Since the flow routing routine affects the entire grid and since it is called every time step (see Fig. 1), a more efficient algorithm for calculating the flow field is required (Coulthard et al., 2007-this issue).

CAESAR uses a "flow-sweeping" algorithm, which calculates a steady-state, uniform flow approximation to the flow field. The new version of the model has a slightly modified implementation of the original flow-sweeping algorithm to accommodate high-resolution grids, where the channel width can easily exceed the grid cell size. Similar to the original CAESAR model, a multi-sweep scanning procedure is applied, except here one scan (*i.e.* one calculation of the flow field) consists of eight sweeps instead of four: two in each of the four primary directions on the grid. During a sweep, the discharge is routed to a range of cells in front, identified through a sweep width, ω (default $\omega=11$). Although smaller values ($\omega=3$ or $\omega=5$) are commonly used in low-resolution CA models (*e.g.*

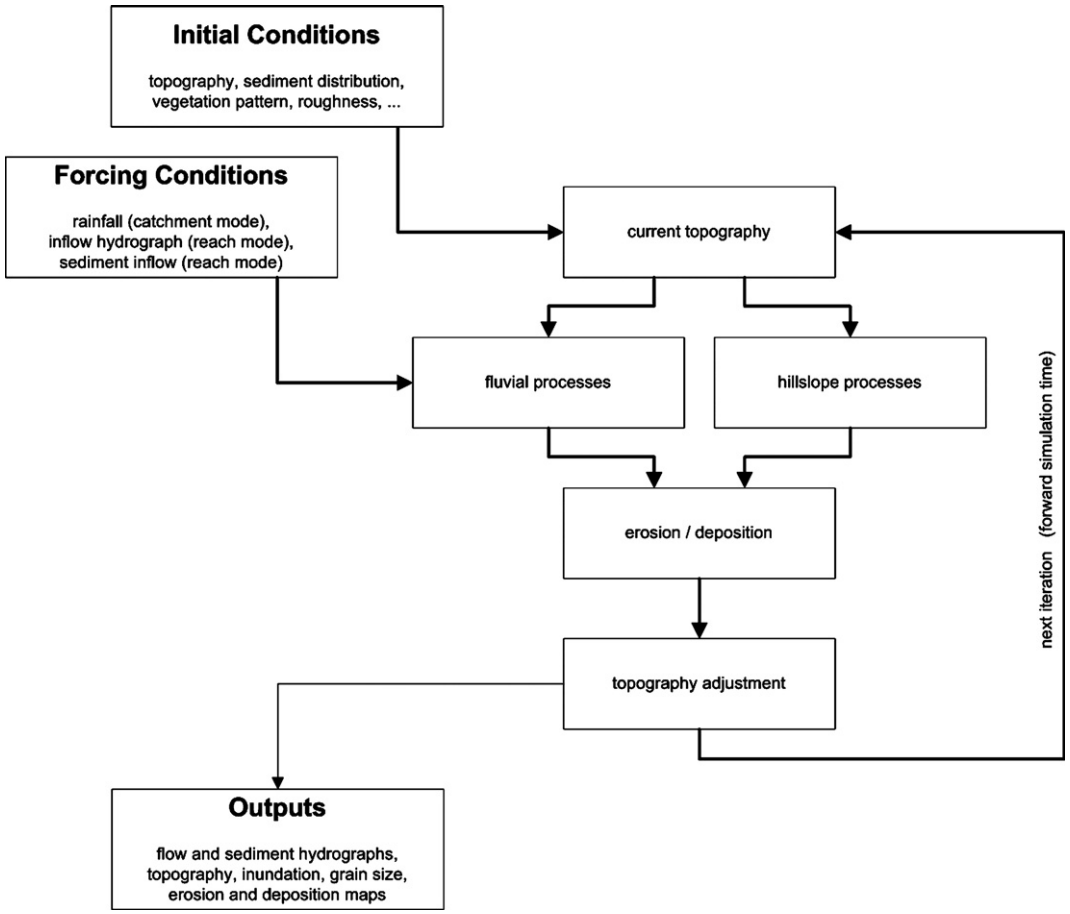

Fig. 1. Conceptual structure of the CAESAR model.

Murray and Paola, 1994; Coulthard, 2001; Thomas and Nicholas, 2002), it was found that, for high-resolution grids, higher values are needed to avoid unrealistic super-elevation of the water level along the outer bank in river bends. Discharge is distributed to all cells within the ω-range according to differences in water elevation of the donor cell and bed elevations in the receiving cell. If no eligible receiving cells can be identified in the sweep direction, *i.e.* if there is a topographic obstruction, then the discharge remains in the donor cells to be distributed in subsequent sweeps (in different directions) during the same scan. Flow depths and flow velocity are calculated from discharges using Manning's equation:

$$Q = UA = \frac{1}{n} h^{2/3} \sqrt{SA} \quad (1)$$

where Q, U and h respectively denote discharge, flow velocity and flow depth, A is the cross-sectional area of the flow ($A = h\ c_w$), S is the average downstream slope, and n is Manning's coefficient. Depending on the topography, the flow depth and flow velocity can be calculated more than once during a scan for a given cell, *i.e.* in different sweeps. When this occurs, the highest calculated flow depth is retained.

The flow-sweeping routine described here is similar in concept to the implicit solution schemes employed in finite difference CFD algorithms, where information (*i.e.* discharge) propagates through the system as each grid point is updated. This propagation of information during an individual time step does not conform to the cellular automaton concept *strictu sensu*, where cells are updated simultaneously and independent of changes in other cells, but was found to be significantly faster than non-propagating explicit implementations. The two main drawbacks of the flow-sweeping algorithm in comparison with CFD-approaches are 1) that it does not conserve momentum, and 2) that it only provides overall flow velocities at each grid point and does not distinguish between primary and secondary flows. This mainly has implications for the calculation of lateral erosion (see below).

2.3. Sediment transport

Although flow is the main driver of the model, all morphological changes result from entrainment, transport and deposition of sediments. CAESAR distinguishes between several sediment fractions, which are transported either as bed load or as suspended load, depending on the grain sizes.

Sediment transport is driven by a mixed-size formula, which calculates transport rates, q_i, for each sediment fraction i (Wilcock and Crowe, 2003):

$$q_i = \frac{F_i U_*^3 W_i^*}{(s-1)g} \tag{2}$$

where, F_i denotes the fractional volume of the i-th sediment in the active layer, U^* is the shear velocity, s is the ratio of sediment to water density, g denotes gravity, and W_i^* is a complex function that relates the fractional transport rate to the total transport rate (see Wilcock and Crowe, 2003, using the same notation). Although Eq. (2), and in particular the expansion of W_i^*, was developed for sand/gravel mixtures only, its use is extrapolated here to include finer non-cohesive sediments (silts). This extrapolation is untested and may be an invalid simplification. Nonetheless, it is deemed a sufficient initial approximation in investigative studies, and it is employed here for convenience rather than accuracy. However, other relations for the entrainment of fine sediments may be required in more detailed studies.

Rates of transport can be converted in to volumes, V_i, by multiplying with the time step of the iteration:

$$V_i = q_i \mathrm{d}t \tag{3}$$

The model uses variable length time steps for each iteration, such that the maximal calculated rate of entrainment, $q_{\max}$, results in a maximal allowed elevation change, $\Delta Z_{\max}$ (default: $\Delta Z_{\max} = 0.1\ L_h$, where L_h denotes the thickness of the sediment layers; see below):

$$\mathrm{d}t = \frac{\Delta Z_{\max} c_w^2}{q_{\max}} \tag{4}$$

This measure assures that the model operates at high temporal resolution (*i.e.* sub-second) during periods of intense geomorphological change, and on coarser temporal resolution (*i.e.* hourly) during periods of relative stability.

Sediments are transported as either bed load or suspended load, which can be selected by the user for each of the grain sizes. Bed load is distributed proportional to the local bed slope:

$$V_{i,k} = \frac{S_k}{\sum S} V_i \tag{5}$$

where the indices i and k respectively denote the sediment fraction and the direction of the neighbour, V is volume and S is slope. Only neighbours with lower bed elevations (*i.e.* $S_k > 0$) are considered (Fig. 2a). Suspended load, on the other hand, is routed according to flow velocity:

$$V_{i,k} = \frac{U_k}{\sum U} V_i \tag{6}$$

where, U denotes flow velocity. All neighbouring cells where the bed elevation is lower than the water elevation in the current cell are considered (Fig. 2b). The calculation

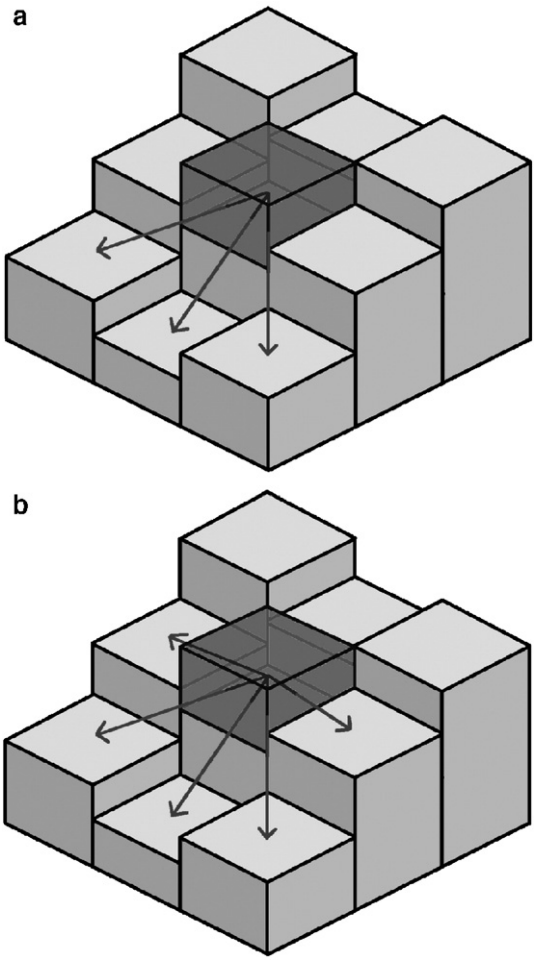

Fig. 2. Routing directions for bed load (a) and suspended sediment load (b).

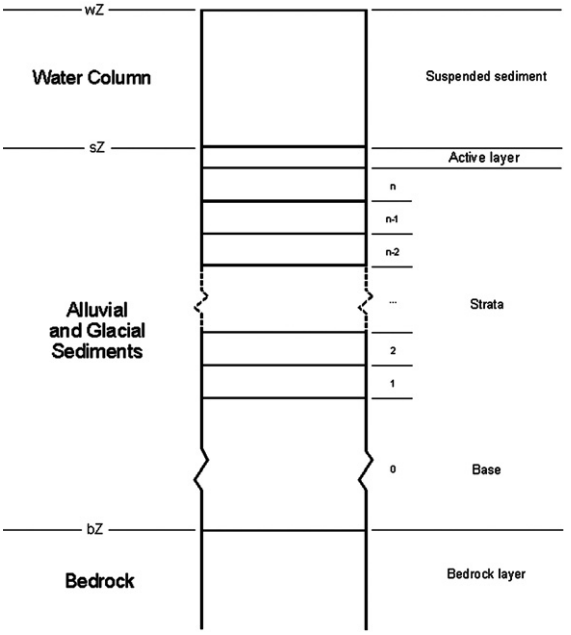

Fig. 3. Sediment layers in CAESAR.

of suspended load routing makes the implicit simplification that suspended sediments are uniformly distributed over the water column at any grid point.

Deposition of sediments also differs between bed load and suspended load. Each iteration, all transported bed load material is deposited in the receiving cells ($V_{i,\mathrm{dep}}=V_i$), where it can be re-entrained in the next iteration. Deposition of suspended sediments, however, is derived from fall velocities, v_i, and concentrations, κ_i, for each suspended sediment fraction:

$$V_{i,\mathrm{dep}} = \kappa_i v_i c_{\mathrm{w}}^2 \mathrm{d}t \tag{7}$$

The remaining volume of suspended load is retained for the next iteration. Eq. (7) implies that some suspended sediment will be deposited every iteration, even where natural flow conditions would prohibit this. However, in these conditions the deposition is only temporary, as it is followed immediately by renewed entrainment of suspended sediment where capacity permits.

Sediment transport in CAESAR is both capacity-limited and detachment-limited. The primary capacity limitation is the transport equation (Eq. (2)), which defines the maximal transport rate for each sediment fraction i at every point on the grid. For suspended sediments, a secondary capacity limitation is employed, such that the total suspended sediment concentration, κ, does not exceed a maximum capacity, $\kappa_{\max}$, after entrainment (default $\kappa_{\max}=0.01$). Detachment–limitation follows from the restriction that, for each sediment fraction i, the transported volume, V_i, must be less or equal to the volume present in the active layer $V_{\mathrm{AL},i}$.

2.4. Sediment layers

The model allows for sediment heterogeneity and keeps track of several (usually 9) user-defined grain size fractions. Selective erosion, transport and deposition of these different fractions will result in spatially variable sediment distributions. Since this variability is expressed not only in the planform dimensions, but also vertically, it requires a method of storing subsurface sediment data. The original version of CAESAR recorded sediment profiles using a multiple active layer system, where each layer is fixed relative to the surface elevation. However, this scheme is physically unrealistic as buried sediments move up and down with topographic changes. Furthermore, it is computationally cumbersome and occasionally causes numerical instabilities. Hence, an alternative approach is adopted herein, using one active layer, multiple buried layers (strata), a base layer and a bedrock layer (Fig. 3). In the current version of the model the bedrock layer is fixed and cannot be eroded. The base layer comprises the lower part of the buried regolith. It has a variable thickness, depending on the number of strata overlaying it. The strata cover the upper part of the buried regolith. They have a fixed thickness, L_{h} (default $L_{\mathrm{h}}=20$ cm), and their position is fixed relative to the bedrock layer. Up to 20 strata can be stored at any cell on the grid. The active layer represents the exposed part of the regolith. It has a variable thickness, between 25% and 150% of the stratum thickness (*i.e.* 5 cm to 30 cm, using the default L_{h} value). Erosion removes sediment and causes the active layer thickness to decrease. If the thickness becomes less than 0.25 L_{h}, then the upper stratum is incorporated in the active layer to form a new, thicker active layer (Fig. 4a). Conversely, deposition adds material to the active layer, causing it to grow. If the active layer becomes greater than 1.5 L_{h} a new stratum is created, leaving a thinner active layer (Fig. 4b). During deposition, the lowest stratum may become incorporated in the base layer, if too many (*i.e.* >20) strata have been created for the cell.

2.5. Lateral erosion

A major new feature in the improved CAESAR model is the implementation of a lateral erosion algorithm. Although it has to be coded explicitly (*i.e.* it does not follow directly from the flow and erosion

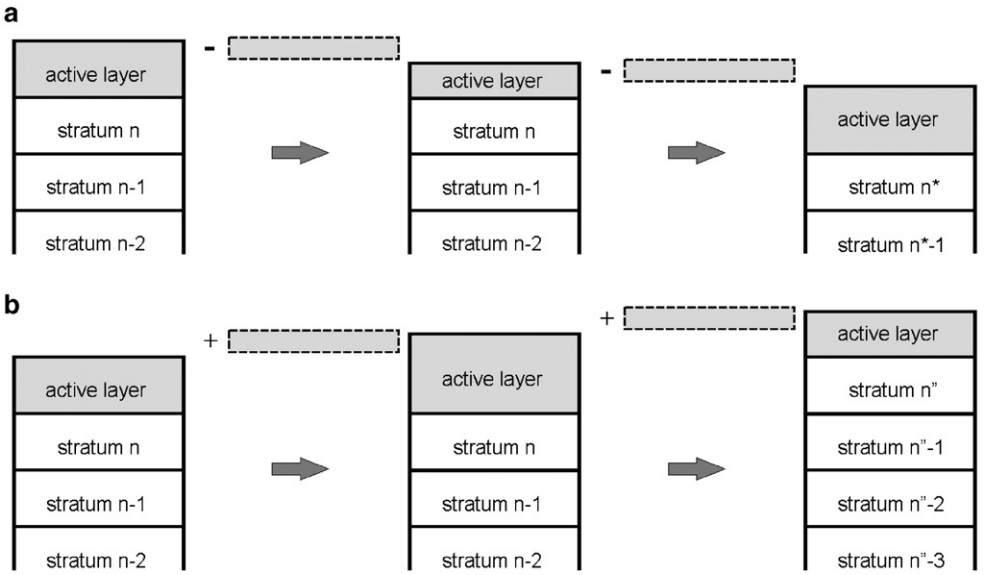

Fig. 4. Dynamics of the active layer during erosion (a) and deposition (b). n denotes the initial number of buried layers. n^* and n'' denote the new number of buried layers; $n^*=n-1$ and $n''=n+1$.

equations), the possibility to simulate lateral erosion in a combined braiding–meandering CA model (like CAESAR) is thought to be a significant step forward in landscape evolution modelling (Coulthard and Van De Wiel, 2006).

The algorithm is split into three conceptual sections: 1) determine the local channel curvature, 2) calculate lateral erosion, and 3) distribute the eroded sediments across the channel. Determining local channel curvature, R_{ca}, is the most time consuming aspect of the algorithm, as several passes are made over the grid in the calculation. In the first pass edge cells are identified. These are defined as dry cells ($h=0$) with at least one wet neighbour ($h>0$) in one of the four primary (*i.e.* non-diagonal) directions (Fig. 5a). In a second pass, a 9-cell filter is passed over the grid (Fig. 5b) to determine inside and outside banks. Where there is an edge cell at the centre of the filter, the number of dry cells is summed, excluding other edge cells. At the same time, the number of wet cells is summed. To avoid false identification of inside banks in near cut-off situations, only the largest connected series of wet cells in the filter is counted. The number of wet cells is then subtracted from dry and this value is assigned to the edge cell at the centre of the filter (Fig. 5c). This value represents a local expression of the radius of curvature, R_{ca}, while its sign identifies inside (negative) and outside (positive) banks. However, the balance of wet and dry cells only provides a very 'rough' measure of curvature, since a meander bend can appear to contain elements of both inside and outside banks, due to the discretization into a cellular grid. Hence, to reduce the roughness of the curvature calculation, a smoothing filter is repeatedly passed over the edge cells, averaging the curvature along the edge cells (Fig. 5d). The radius of curvature term thus obtained is a dimensionless (scaled to grid cell size) approximation of the actual radius of curvature, R. A series of numerical experiments showed significant relation between the R_{ca} and R ($r^2=0.9998$; $n=6$; Coulthard and Van De Wiel, 2006):

$$R = 2.13|R_{ca}|^{-1.08}c_w \tag{8}$$

The method outlined above shows a sensitivity to the number smoothing passes. For near-circular bends the optimal number of smoothing passes was found to be 5 (Coulthard and Van De Wiel, 2006). However, this number may increase when applied to irregular meander bends, although usually no more than 10 smoothing passes are required.

After local radii of curvature have been determined for each edge cell, the lateral erosion rates, ζ, are calculated from a simple relation:

$$\zeta = E_{ca}R_{ca}U_{nb}h_{nb} \tag{9}$$

where E_{ca} is a bank erosion coefficient, and U_{nb} and h_{nb} respectively denote the near-bank flow velocity and water depth in the wet cells neighbouring the edge cell. This approach is similar to the method employed in vector-based linearized meander models (Ikeda et al.,

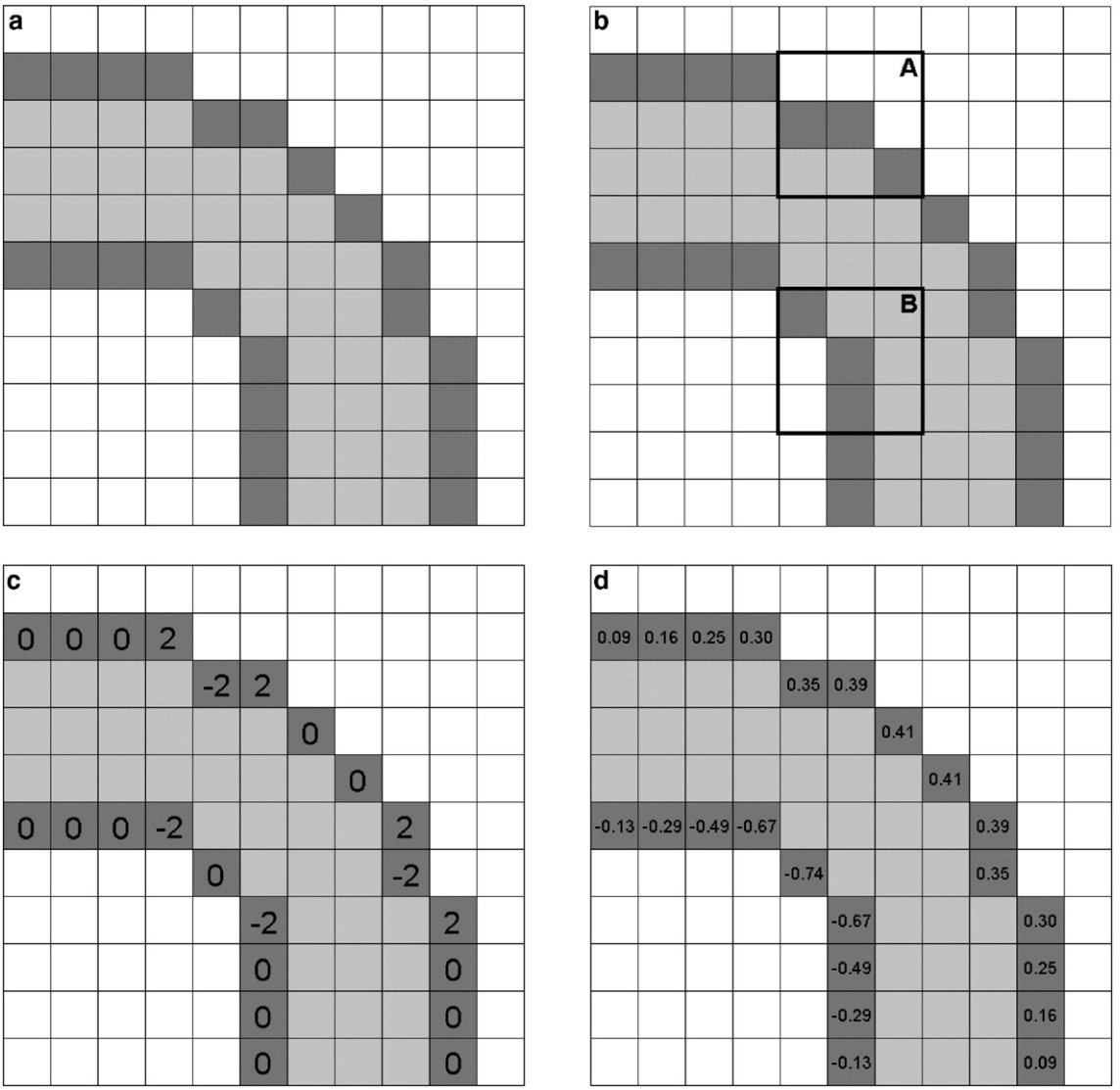

Fig. 5. Example of calculation of the curvature coefficient as used in the lateral erosion algorithm. a. Determination of edge cells (dark) as neighbours of channel cells (light). b. Passing of a 3 × 3 filter over edge cells, counting number of dry cells and wet cells in filter. c. Difference between wet and dry cells is assigned to the centre of the filter. d. Repeated smoothing removes spurious 'straight' sections (assigned 0 in (c)).

1981; Blondeaux and Seminara, 1985; Johanneson and Parker, 1989; Sun et al., 2001), which relate lateral bank migration rates, ζ, to near-bank flow velocity which in turn is a function of channel curvature and cross-sectional averages of flow depth, flow velocity, and roughness. However, the linear relation to curvature expressed in Eq. (9) is a simplification of reality. In natural rivers the lateral erosion rate ζ is a more complex function of the channel's curvature-over-width ratio (Nanson and Hickin, 1983). For the current analysis this relation is neglected, as work is underway to develop an efficient CA algorithm for determining the width of arbitrary channels.

The linearized meander models, by moving the channel position laterally and maintaining channel width, implicitly assume that the amount of deposition on the inside edge of a bend roughly equals the amount of erosion on the outer bank — an assumption which has been shown to be incorrect (Lauer and Parker, 2005). Unlike the linearized meander models, CAESAR does not assume a fixed channel width, but determines deposition along the inside bank from the model's automaton rules. Ideally, the model should not need to be told where to deposit sediment in order to develop the inside of a bend. Rather, it should be preferentially deposited there due to the hydraulic conditions within

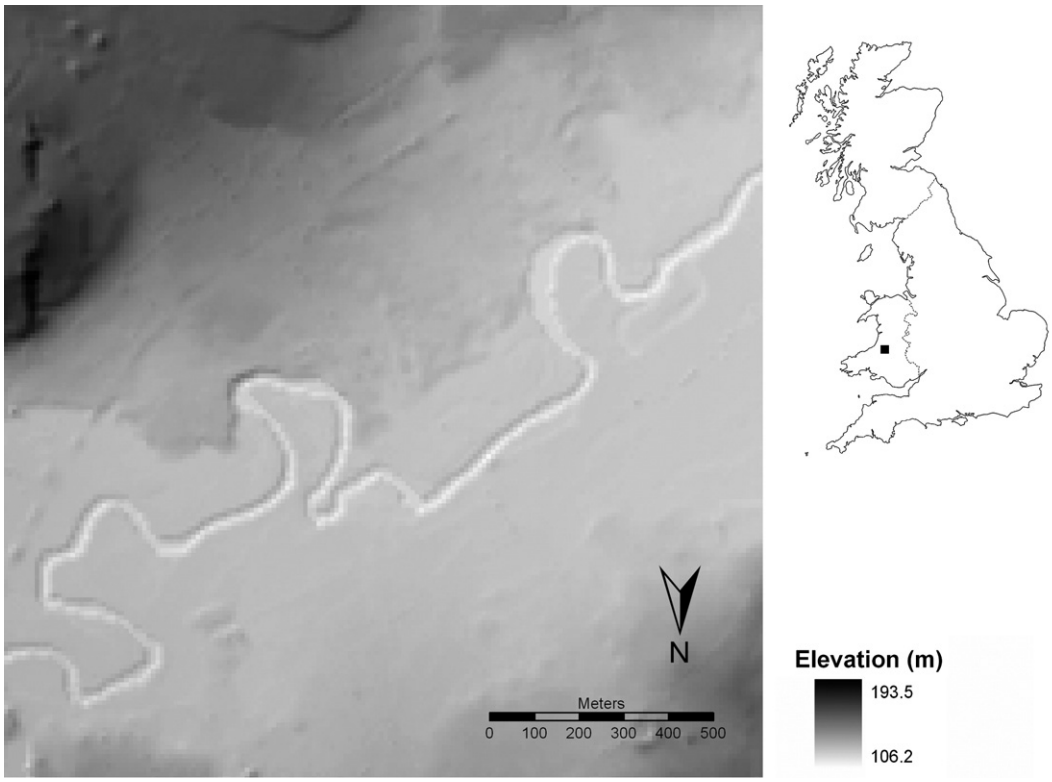

Fig. 6. DEM of the Teifi reach. Note that the DEM is rotated such that the flow is from left to right.

the channel. Unfortunately, in most cellular models there is no representation of secondary circulation and sediment is routed according to local downward slopes (see above). Thus, sediment cannot be moved onto point bars using the existing automaton rules, and an additional routine for explicit lateral redistribution of the eroded sediments must be included. In CAESAR, this is achieved through the use of a cross-stream gradient. One of the benefits of the curvature algorithm is that it assigns a curvature value to both the outside and inside banks, respectively using positive and negative values for R_{ca}. This property can be used to determine a cross-stream gradient of curvature, by applying an averaging filter across all wet cells to interpolate the values across the channel. This cross-stream gradient of curvature is then used to calculate a lateral sediment flux, ψ_n:

$$\psi_n = a(R_{ca,n} - R_{ca,n-1})h_n \quad (10)$$

where n and $n-1$ respectively denote the donor cell and the receiving cell, a is a coefficient and h is the flow depth. It should be noted, however, that there is no physical basis for assuming that cross-channel gradient of curvature would govern lateral sediment distribution. Nonetheless, in the absence of secondary flow representation it is a useful technique for forcing lateral sediment distribution within the CA framework. In effect, through Eq. (10) we are simulating the symptoms of lateral erosion, rather than the causes.

3. Examples

Three simulations were carried out on a 4.2 km reach of the River Teifi, near Lampeter, Wales. A 10 m resolution DEM for the reach was generated from LiDAR data (Fig. 6). The Teifi is a meandering river (sinuosity = 2.0) with irregular meander loops. Several paleochannels exist on the floodplain, mainly on the north of the channel. On the southern side, a large alluvial fan covers part of the floodplain and is gradually being eroded by the

Table 1
Simulation setup

Simulation	Duration [days]	Q [m^3/s]	E_{ca} [–]	ω [–]
T1	n/a	20; 100; 200	0	11
T2	171	20; 200	0	11
T3	3	20	0.0001	11

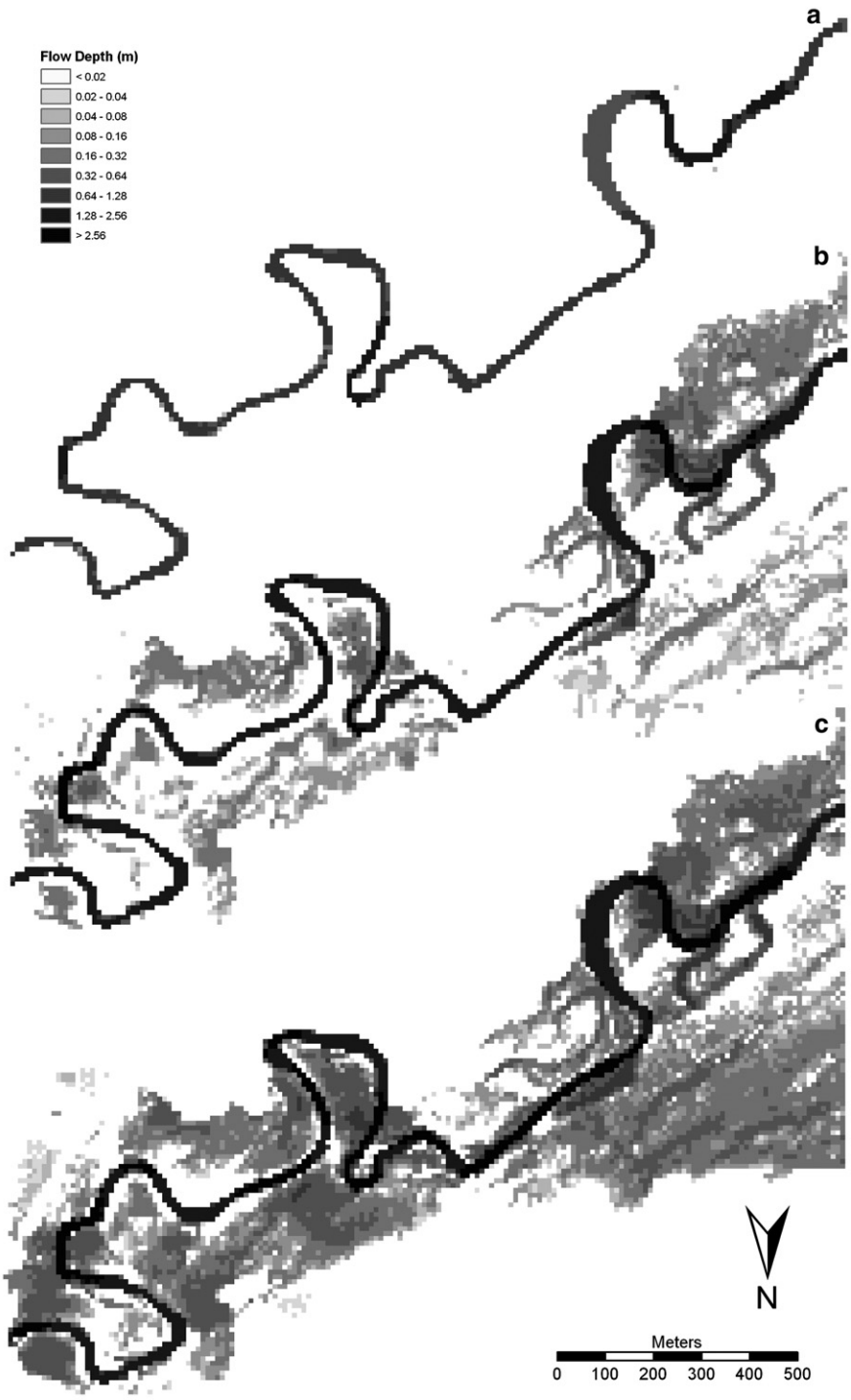

Fig. 7. Flow depths at different discharges in simulation T1. a. 20 m^3/s. b. 100 m^3/s. c. 200 m^3/s. Flow is from left to right.

migrating river channel. Although LiDAR's vertical resolution is small enough to resolve paleochannels on the floodplain, it is unsuitable for defining the channel bed, since it records the water surface elevations rather than the bed topography. Hence, an artificial channel bed was introduced by lowering the DEM by 2 m for channel cells, effectively creating rectangular channel cross-sections for the entire reach.

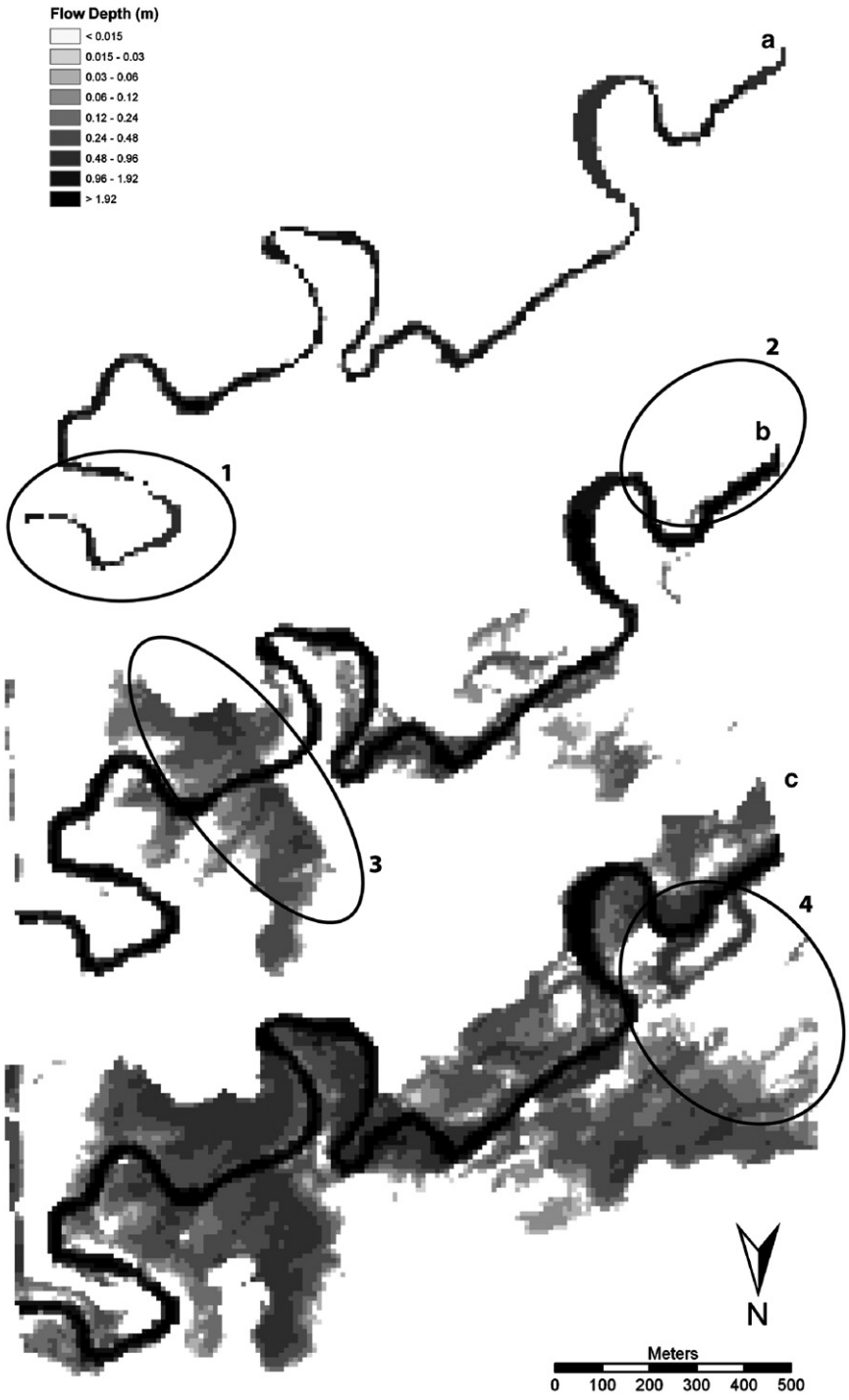

Fig. 8. Flow depths at different discharges in HEC-RAS simulations. a. 20 m^3/s. b. 100 m^3/s. c. 200 m^3/s. See main text for explanation of highlighted areas (1–4). Flow is from left to right.

As the main purpose of these simulations is to perform a preliminary evaluation of the different aspects of the new CAESAR model, the numerical setup of the simulations was chosen to accelerate the development of particular morphological features in the landscape, rather than reflecting natural conditions at the site (Table 1). Simulation

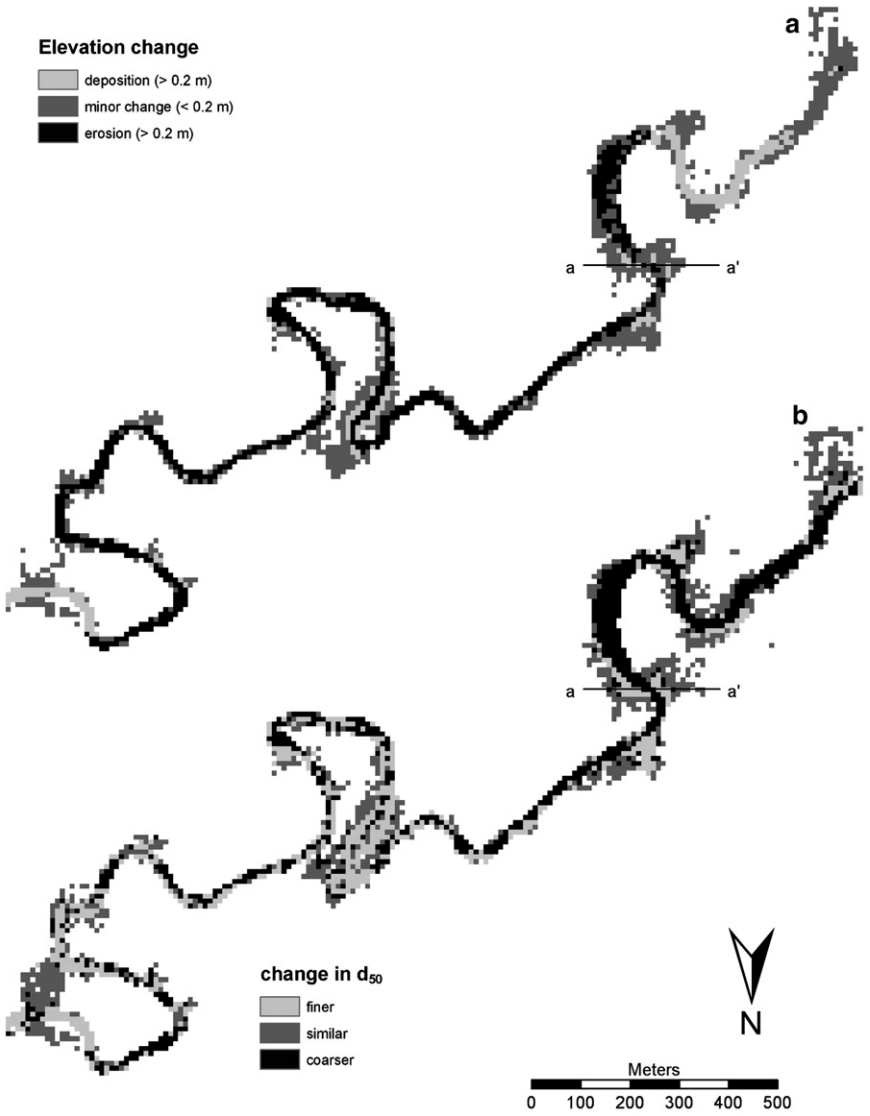

Fig. 9. Elevation change (a) and median grain size in the active layer (b) at the end of simulation T2. Flow is from left to right. Cross-section a–a′ is shown in Fig. 10.

T1 was designed to show the flow routing abilities of the model for in-channel and overbank flow conditions and does not incorporate sediment movement. Simulation T2 focusses on overbank deposition, and incorporates frequent flooding — alternating 24 h of in-channel flow (20 m^3/s) with 24 h of overbank flow (200 m^3/s). Simulation T3 was designed to show bank erosion and channel migration, and employs an erosion coefficient, E_{ca}, which is several orders of magnitude too high, in order to accelerate the bank erosion process. Clearly, these unrealistic simulation configurations impose severe restrictions on the quantitative interpretation of the results. However, we consider that these simulations provide sufficient information to perform a preliminary qualitative evaluation of the model's abilities and limitations.

In simulation T1, three different discharges are run across the DEM. Low-discharge flows are contained within the channel banks (Fig. 7a), while high-discharge flows inundate the floodplain (Fig. 7b and c). Overbank flooding is more extensive on the northern side of the channel in this reach of the Teifi, due to the raised terrain of the alluvial fan to the south. Floodplain topography also controls the pattern and depth of inundation, with paleochannels and other low lying areas more likely to be flooded. Although these result may appear trivial, they represent notable improvements

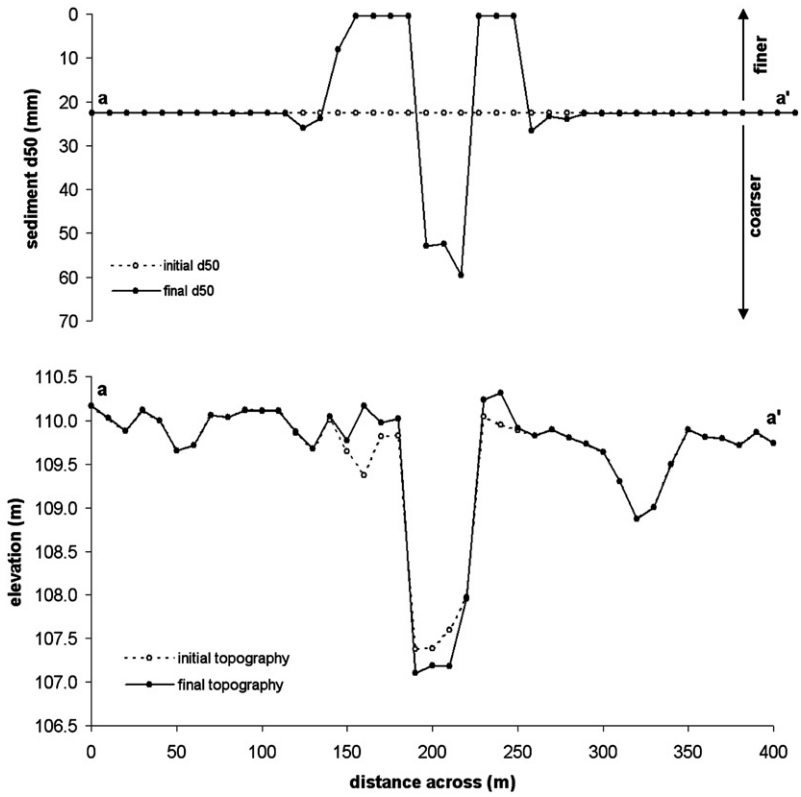

Fig. 10. Cross-sectional profile of elevation (bottom) and median grain size (top) across two splays, formed in simulation T2. Location of the cross-section is shown in Fig. 9.

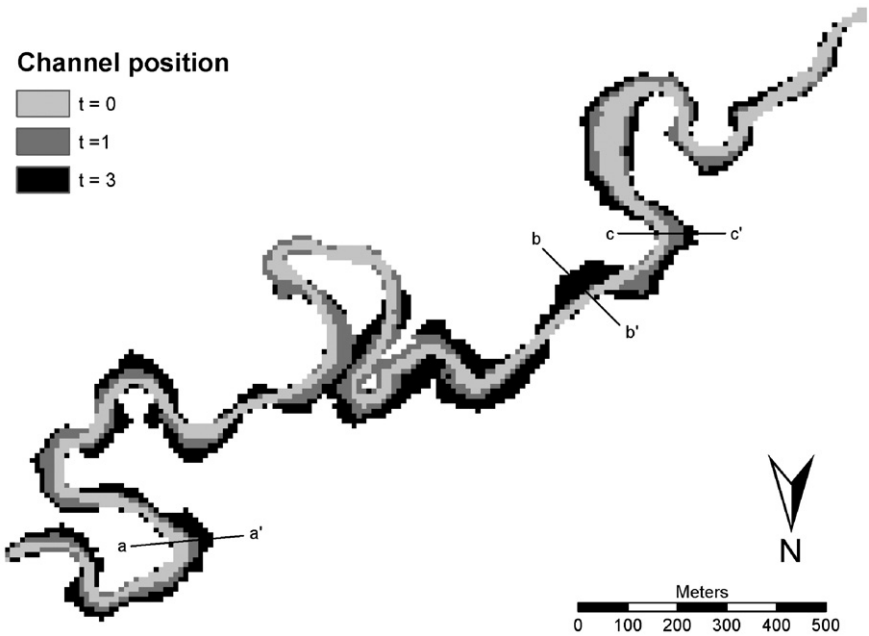

Fig. 11. The channel's planform position during simulation T3, at the start of the simulation (light grey), after 1 day (dark grey) and at the end of the simulation (black). Flow is from left to right. The cross-sections are shown in Fig. 12.

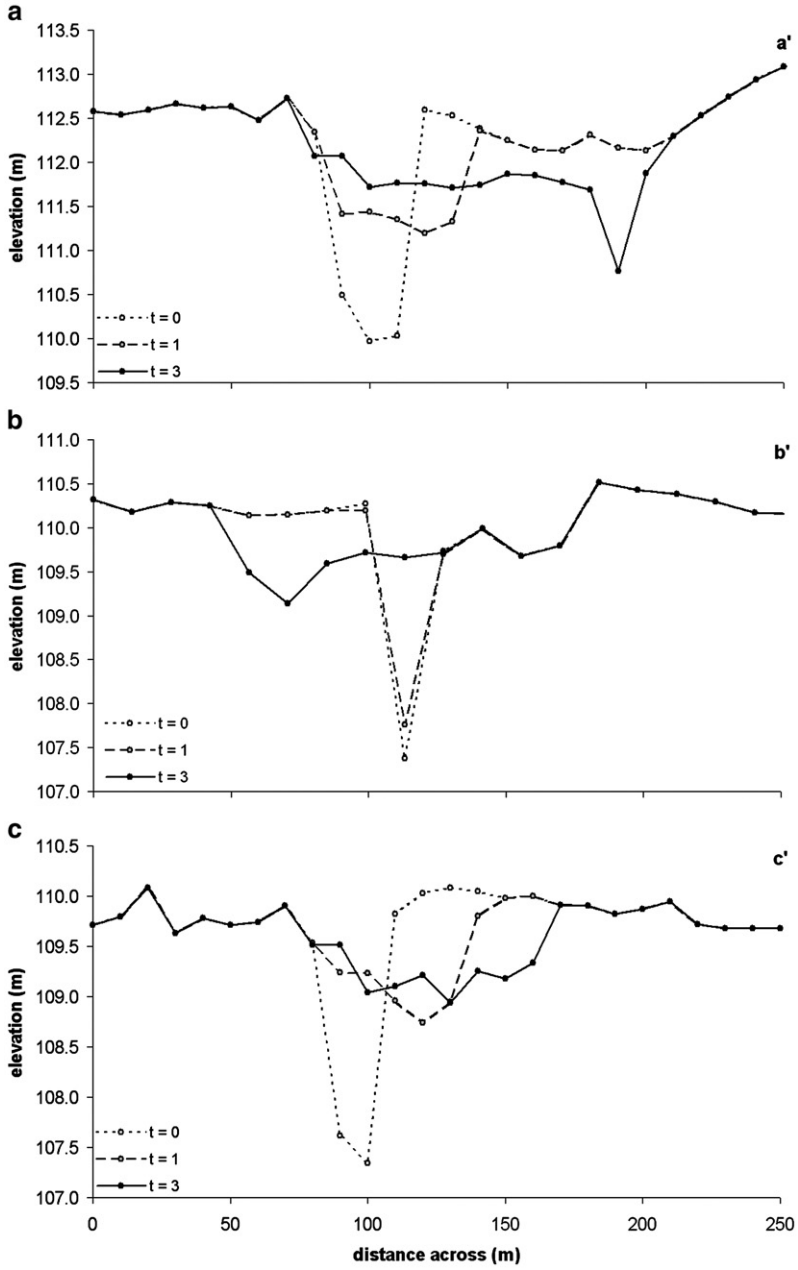

Fig. 12. Lateral migration of the channel at three cross-sections. Profiles are shown for initial (t=0 days), intermediate (t=1 day) and final (t=3 days) topographies. Location of the cross-sections is shown in Fig. 11.

for cellular automaton flow algorithms — particularly, the ability to route flow through a high-resolution meandering channel (see Coulthard et al., 2007-this issue).

Fig. 8 shows the inundation patterns predicted by a 1-dimensional model (HEC-RAS v3.1; US Army Corps of Engineers, 2003). Although the broad patterns of inundation are similar in both models, *i.e.* in-channel flow at 20 m^3/s and partial flooding at 100 m^3/s and 200 m^3/s, there are some notable differences as well, particularly in the spatial occurrence of the flooding. These differences can be attributed to several factors. First, the channel morphology differs slightly between the two models. Due to a conversion from a raster DEM to TIN (HEC-RAS requires a TIN), the channel is narrower in the HEC-RAS simulations (Fig. 8a[1]). Second, floodplain inundation might spread from a

limited number of spill points, particularly for near bankfull flow conditions. Due to cross-sectional spacing, these spill points might not be picked out by HEC-RAS (Fig. 8b[2]). Finally, CAESAR applies local routing of discharges at every point on the DEM. HEC-RAS, on the other hand, routes flow from cross-section to cross-section. As a result, predicted inundation pattern can change rapidly from one cross-section to another (Fig. 8b[3] and c[4]).

Simulation T2 shows that erosion and deposition of sediments, according to Eqs. (2)–(7), not only alter the topography of the reach (Fig. 9a), but also affect the sediment distribution, both in-channel and on the floodplain (Fig. 9b). Under the conditions of simulation T2, the channel is incising for most of its length (Fig. 9a), although there are two smaller sections of in-channel deposition: one at the upper end of the reach, and one at the final bend near the lower end of the reach. Additionally, at the end of the simulation most of the channel bed consists of coarser sediments (Fig. 9b). This suggests that most of the in-channel incision results from the selective entrainment of finer sediments. Hence, the model reproduces the processes leading to bed armouring. The deposition at the upper end of the reach, consisting of both fine and coarse sediments (Fig. 9)), is a boundary condition effect, reflecting the system's response to a large influx of sediments at the inlet. The second in-channel deposition area consists mainly of coarse bed load material (Fig. 9), and is caused by a step in the channel bed topography at the apex of the second to the last meander bend. This step is an artefact of the LiDAR data and the channel definition. However, here CAESAR incises immediately upstream of the step, and deposits coarse material downstream of the step, effectively smoothing the bed perturbation. The fine sediments which are entrained from the channel bed are either washed out of the system, or are deposited on the floodplain during the overbank floods. This leads to the formation of both levees and splays (Fig. 9a). There are other areas of subtle overbank deposition — for example in paleochannels — but these are not revealed due to the shading scheme used in Fig. 9. A cross-section profile through two opposite splays clearly shows that the depositional features consist of fine sediments, while the erosion of the channel results in bed armouring (Fig. 10). All of these results are consistent with those that would be expected from a natural stream, and demonstrate how the combination of flow routing, erosion and deposition with several grain size fractions, active layers and suspended sediment all combine to produce incision, deposition, splays and levees. Furthermore, Figs. 9 and 10 demonstrate how grain size patterns in bed armouring and the deposition of overbank fines as levees reflect the trends found in real rivers.

There is no overbank flow in simulation T3, due to the low-discharge flow (Table 1). However, lateral erosion still occurs, in spite of the low-discharge conditions, largely due to the exaggerated value for the bank erosion coefficient. Fig. 11 shows the channel position at different stages of the simulation. It can be seen that most of the lateral erosion occurs on the outer banks of the bends, which is a direct consequence of the structure of the bank erosion algorithm. However, it is worth noting that the channel has not migrated southward where the alluvial fan cannot be easily removed. Cross-sectional profiles (Fig. 12) illustrate that the lateral erosion is not uniform over time. Temporal variations in lateral erosion, even at constant discharge, are due to changes in channel configuration, and hence curvature and flow field, as the simulation progresses. As a result of the lateral channel migration, several bends are close to forming cut-offs. However, the current algorithm does not deal well with cut-offs, as the concept of wet cells and dry cells to determine inside and outside bends becomes invalid for near-touching banks. Additionally, the high influx of laterally eroded sediments from the banks could not be evacuated by the low-discharge flow in the channel, thereby gradually choking the channel with sediment. Hence, the simulation was halted before cut-offs occurred, *i.e.* after three days. Nonetheless, simulation T3 shows that lateral erosion can be achieved in cellular automaton models. However, it is unclear from this simulation whether the lateral movement represents channel widening or channel migration. There is little lateral deposition opposite the eroding banks (Fig. 12), which indicates that the processes leading to point bar formation is currently inadequately represented in the model.

4. Discussion and future uses

The results from the sample simulations, using hypothetical numerical parameters and boundary conditions, illustrate that the model is, in principle, able to replicate alluvial processes and forms such as channel incision, bed armouring, splays and levee formation, and meander bend migration. These results are not presented as definitive, but as a preliminary qualitative evaluation. Importantly, these simulations were carried out over a short period of time. For example, scenario T2 (simulating erosion and deposition over several days of high and low flows) took 42 h to complete on a desktop PC and the solutions of the flow fields in Fig. 7 took a fraction of a second. This is one of the key

advantages of reduced complexity cellular models such as CAESAR. By using simplifications of flow equations coupled with sediment transport relations we can rapidly simulate geomorphic processes over medium time scales and detailed spatial resolutions. Thus, the model is not restricted to simulating a single flood over a short stretch of the river. This raises the potential for many new and exciting applications.

As mentioned in the Introduction, CAESAR can operate in catchment or reach mode. This allows the catchment above a study reach to be simulated using the catchment mode CAESAR. Using the inputs of an hourly rain fall record and the DEM, CAESAR will simulate erosion and deposition across the whole catchment and generate a file of water and sediment outputs (in multiple grain sizes) produced at the basin outlet. This can then be used as an input file for a more detailed CAESAR model of a reach, as illustrated in Fig. 13. This linked catchment-reach modelling approach has several useful advantages. Firstly, it reduces the boundary condition requirements. Frequently researchers are interested in one reach of a catchment. Yet a reach is just one part of a river, and what occurs within a reach may well be defined by the boundary conditions, *i.e.* by the topography and shape of the reach itself, but more importantly by what lies above and below the reach, and what quantities of water and sediment are fed into it. Ideally, water and sediment samplers should be placed above a study reach, so that a record of actual inputs can be determined, but this is rarely feasible, particularly for long-term simulations. The linked catchment-reach strategy allows the catchment model to simulate all the erosion and depositional processes occurring upstream of the reach — effectively generating its own boundary conditions for the reach-scale simulations. Secondly, the split method allows the catchment to be run at a coarser spatial resolution (*e.g.* at 20 to 50 m grid cells) yet the reach to be run at a finer resolution (*e.g.* 10 m, as here) where more detail is required. This can considerably decrease model run times, as there is a greater than exponential increase in speed with a linear increase in grid cell size. Finally, the split catchment-reach approach facilitates parallelization: reach and catchment models can be run on separate machines, increasing the speed of operation. Furthermore, the catchment upstream of a reach may be split into several sub-catchments and further parallelized.

The developments in the new CAESAR model presented here provide a significant improvement over the previous version and other landscape evolution models. By incorporating lateral erosion, suspended sediment and multiple grain size fractions, CAESAR now covers many of the processes pertinent to the development of alluvial environments. However, with the integration of these new, yet arguably important, processes several practical and more philosophical questions can be raised. How important are these processes for the model's operation? And relating these directly to fluvial landscape evolution, how important are they for the development of river systems? Are we in danger of over-complicating fluvial CA models? By introducing more and more detailed processes into CA models, are we starting to blur the lines between complex and reduced complexity models? Are we making the CA models more accurate or more unwieldy? If the latter is the case, then ironically they could become as complex as the CFD models they were designed to simplify.

In our attempt to answer some of these questions we must distinguish between two apparently different approaches to computational landscape evolution modelling (Murray, 2003; Werner, 2003; Coulthard et al., 2007-this issue), and indeed computational modelling in general. In the first instance there is the reductionist approach, in which a system is broken down in smaller components and processes, which are modelled in detail (*e.g.* sediment mobility is reduced to four processes: exertion of shear by the fluid, sediment entrainment due to excess shear, subsequent transport by the flow, settling of particles due to gravity). Subsequently, larger-scale structures (*e.g.* point bars, pools and riffles, river terraces) emerge from interactions between the smaller-scale components. The three main criticisms of this approach are: 1) it is often impossible or impractical to simulate all the smaller components of a system, forcing a subjective selection of components by the modeller, based on an *a priori* evaluation of their perceived relative importance; 2) interactions between components do not necessarily follow from their description, but may need to be described on a higher level; and 3) the reductionist step is in principle never-ending, *i.e.* each individual component can be broken down in ever smaller components (*e.g.* flow can be broken down into downstream, lateral and vertical components, each subject to turbulent eddies, which consist of smaller eddies, which are due to local differences in fluid density, and so on), until one arrives at atomic or sub-atomic level, which most geomorphologists would agree is an absurd level at which to try and explain landforms.

In the second instance there is the holistic approach to modelling, in which the system is simulated as a whole, *i.e.* larger-scale forms are modelled directly, without reference to the smaller-scale components. Such models generally try to establish the simplest rules that replicate the observed behaviour of the system. The main assumption of these models is that smaller-scale processes do not matter much to the systems overall behaviour.

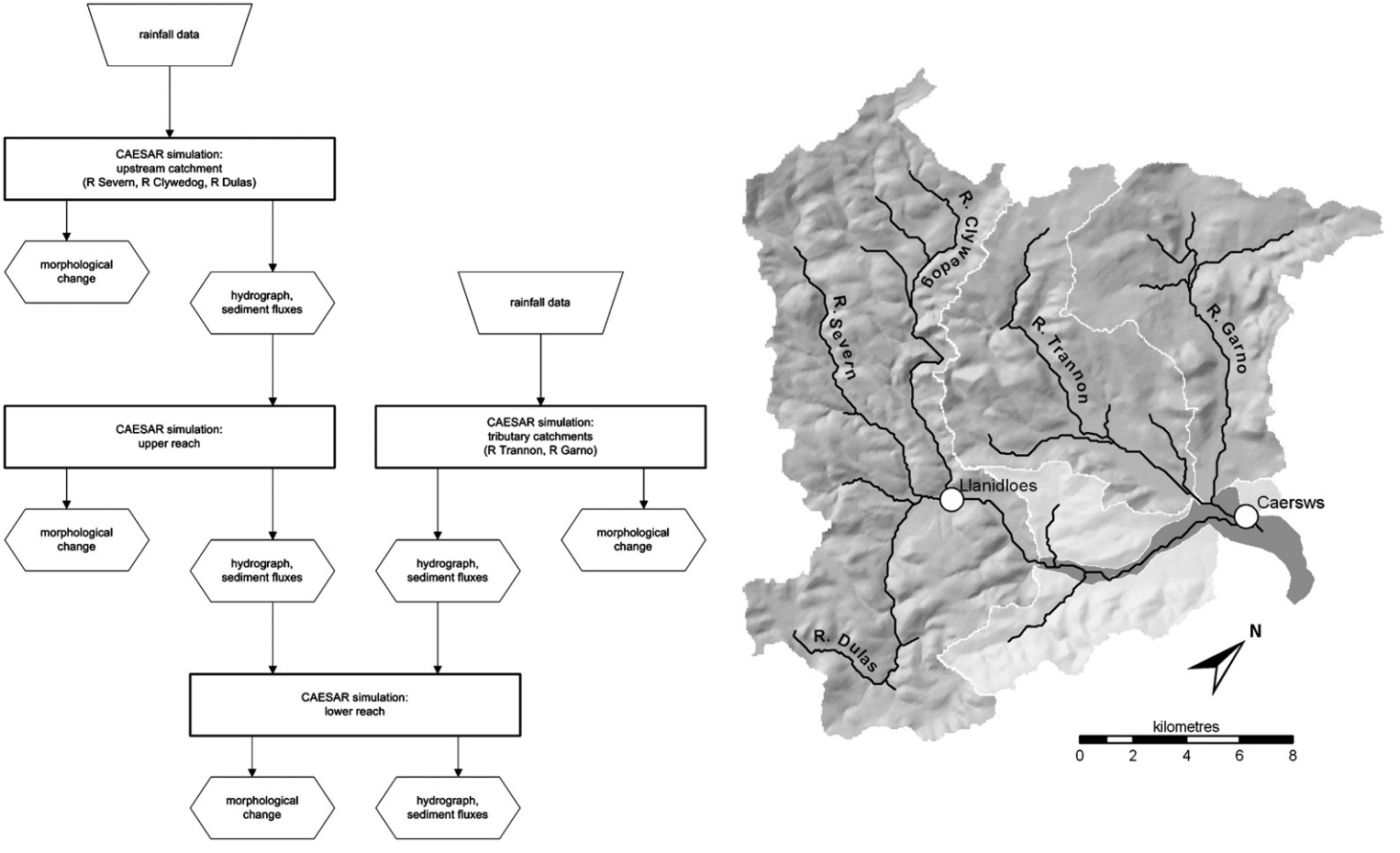

Fig. 13. Example of a split catchment-reach setup for a sequence of CAESAR simulations on the River Severn, Wales. The flow diagram describes the procedure, and the map indicates the two catchments feeding into the reach runs around Caersws.

However, this assumption is unverified and the principal danger of the holistic method is that by simplifying the system too greatly, we may lose some of the detail or 'noise' in the system that may be vital to its evolution.

Importantly, despite their fundamental differences the reductionist and holistic approaches have one thing in common: emergence. In the reductionist models, larger-scale features emerge from the interaction between smaller-scale components and processes, whilst in holistic models system complexity emerges from simple behavioural rules. Without emergence nothing could be learned from either reductionist or holistic models. However, the different nature of the emergence in the two approaches largely determines what can be learned from the models, and what questions can be asked from them (Bras et al., 2003; Murray, 2003). Reductionist models tend to be used for detailed *prediction* in scenarios where the processes and their interactions are well understood. For example, a reductionist CFD modelling approach can be applied to predict inundation pattern and flow field on a floodplain for a particular flood event (*e.g.* Nicholas and Mitchell, 2003; Hesselink et al., 2003). Holistic models tend to be used in more *exploratory* studies, where it is attempted to improve understanding of overall system behaviour. For example, for a long time braiding was considered a combination of many factors. Yet Murray and Paola (1994) showed that a cellular model, iterating a few simple rules describing the distribution of flow and sediment, could simulate seemingly realistic braid patterns. The Murray and Paola model perfectly illustrates the difference between the two approaches in that it helps us to understand the overall dynamics of braided river systems, but cannot predict the precise position on the floodplain of a particular braid anabranch.

However, it should be noted that the reductionist and holistic approaches operate across a continuum (Murray, 2003; Werner, 2003) and in practice very few models are purely holistic or purely reductionist, with most located somewhere in between. Here, CFD models tend more towards reductionism, while most CA models tend towards the holistic approach, but neither are exclusively so.

CAESAR is placed somewhere between these two positions. Like the Murray–Paola model of river braiding (Murray and Paola, 1994), it is based on the reduced complexity concept, where a few simple rules of water and sediment distribution replicate the planform behaviour of braided rivers. However, the inclusion of additional smaller-scale processes (*e.g.* improved flow model, bank erosion, sediment heterogeneity, suspended sediment transport) nudges CAESAR a little closer towards the reductionist end of the scale. This puts it in a precarious position. Unlike the algorithms used in CFD models, the CA rules of CAESAR are not complex enough to be based on first principles or direct derivations thereof, but instead rely upon (largely) empirical relationships. Conversely, the rules are possibly too complex for CAESAR to be considered just a simple hypothesis-testing model.

A good example of this is the application of CAESAR to braided river systems. For example, if we wish to see whether starving the system of sediment will change the braid index of a reach, CAESAR might be considered too unwieldy, and simple cellular braided river models, like those of Murray and Paola (1994) or Thomas and Nicholas (2002), might be more appropriate. Whilst CAESAR is able to replicate the results of the simpler braided river models, it adds levels of complexity (*e.g.* multiple grain sizes, improved flow model, suspended sediment transport) that may provide enhanced realism, yet may not contribute greatly to the overall outcome of the simulations. However, one of the benefits of CAESAR is that it can be used to test the holistic assumption that smaller-scale processes do not have a significant impact on the overall behaviour of the system, by selectively activating different layers of complexity. The other important advantage of CAESAR over the simpler braided river models is that the additional detail in CAESAR allows additional questions to be asked. For example, if we wish to see how the starvation of sediment affects surface grain size distribution, the CAESAR would have to be used, as the simpler models do not account for sediment heterogeneity. Thus, although the nudge towards reductionism might make the model cumbersome for some purposes, it opens up new lines of investigation in other areas. Such developments are perhaps inevitable, as the next step once a model has been shown to operate successfully is to add features to allow it to explore new circumstances. This is certainly the case in the development of the CAESAR model from 1996 to 2006. There is always scope for further reductionist refinement and inclusion of additional processes. For example CAESAR does not include processes of weathering, groundwater effects or surface structuring, although all of these could be argued to have an impact on landscape evolution.

Another fascinating research area that may be explored with the new CAESAR model is that of braided and meandering channels. Currently, there are no cellular models which can simulate both braiding and meandering. However, the addition of a lateral erosion scheme to a cellular model that is capable of simulating braided rivers raises the prospect of modelling how rivers move from braided to meandering and back, and what controls this

transition (Coulthard and Van De Wiel, 2006). Again, this possibility arises from the incorporation of additional processes, such as bank erosion, in the model.

However, the introduction of additional processes in the model also introduces new parameters and increases the data requirements of the model. CAESAR's sensitivity to these additional sources of uncertainty has not yet been investigated. Additionally, we have to be careful how we simplify models. For example, sediment transport relations may not be fully accurate (Gomez and Church, 1989; Coulthard et al., 2007-this issue), but they are based on basic principles of physics, *i.e.* the energy of the flow can entrain and move sediment. However, our lateral erosion algorithm is based upon the radius of curvature and, hence, is simulating the symptoms rather than the causes of lateral erosion. An allegory is to calculate the erosive capacity of water based upon the darkness of the water colour in imagery, which may be a proxy for water depth (an important variable in the calculation of shear stress), but is not directly related to erosion. Furthermore, the structure of process representation also has to be carefully considered. For example, our use of an active layer system, with buried strata of equal thickness appears a good way of integrating the multiple layers within a stratigraphy within the model. However, it is unrealistic in that for natural river systems neither the river bed nor the floodplain will normally consist of multiple layers of equal thickness. Such simplifications mean that CAESAR is too simple to be used for the kind of detailed predictive purposes required in, for example, river engineering applications.

Thus, in spite of the steps towards reductionism and the increased complexity of the model, CAESAR remains a reduced complexity model, whose main purpose is the exploratory investigation of landscape evolution dynamics.

5. Conclusion

This paper has introduced new or improved techniques for representing alluvial processes in a cellular automaton landscape evolution model. These include: 1) improved rules for multi-directional flow routing allowing representation of flow in meandering channels and over complex topographies; 2) new rules for sediment transport distinguishing between bed load and suspended load; and 3) a new cellular automaton algorithm for lateral erosion.

Sample simulations, using hypothetical numerical parameters and boundary conditions, have been run on a reach of the River Teifi. The results from these simulations illustrate that the model is, in principle, able to replicate alluvial processes and forms such as channel incision, bed armouring, splays and levee formation, and meander migration. The emergence of these processes and forms from simple local automaton rules is a promising indicator of the model's ability to simulate long-term larger-scale alluvial landscape evolution. However, the unrealistic conditions of these preliminary simulations, as well as their small spatial and temporal scale, preclude quantitative interpretation of the results. Further simulations, with realistic numerical parameters and flow conditions, are required to investigate the long-term behaviour of the model in natural environments.

Although the new CAESAR model sits between the more complex reductionist models and the simpler holistic models — being too simple for detailed prediction yet too complex for pure exploratory research — the inclusion of additional layers of complexity in the model has several benefits. First, it allows more detailed simulation of in-channel and floodplain morphology. Second, the linked catchment-reach approach improves computational efficiency, by focussing on detail where possible. Third, and arguably most important of all, it allows to open up new lines of exploratory enquiry, for example into the effects of climate change on alluvial landform development, or into the emergence of channel pattern type in relation to sediment and flow regime at time and space scales that are pertinent to modern studies. This additional detail in process simulation also increases the model's complexity, adding more parameters to model and increasing data requirements. Further investigation of the influence of the parameters and of impact of the additional processes on the overall outcome of the simulations, is required to establish if the trend towards increased reductionism in reduced complexity cellular models is warranted.

Acknowledgements

MJVDW was funded by NERC grant NER/A/S/2001/00454 awarded to TJC. We thank the two anonymous referees for their constructive criticism. We would also like to thank Drs Gez Foster, Jeremy Walsh, Joe Wheaton and Clare Cox who have all contributed to the development of the CAESAR model. The CAESAR model used in this paper can be downloaded for free from http://www.coulthard.org.uk.

References

Bates, P.D., Lane, S.N. (Eds.), 2000. High Resolution Flow Modelling in Hydrology and Geomorphology. Advances in Hydrological Processes. Wiley, Chichester. 374 pp.

Blondeaux, P., Seminara, G., 1985. A unified bar-bend theory of river meanders. Journal of Fluid Mechanics 157, 449–470.

Bras, R.L., Tucker, G.E., Teles, V., 2003. Six myths about mathematical modeling in geomorphology. In: Wilcock, P.R., Iverson, R.M. (Eds.), Prediction in Geomorphology. Geophysical Monograph. American Geophysical Union, Washington, DC, pp. 63–79.

Coulthard, T.J., 2001. Landscape evolution models: a software review. Hydrological Processes 15, 165–173.

Coulthard, T.J., Van De Wiel, M.J., 2006. A cellular model of river meandering. Earth Surface Processes and Landforms 31, 123–132.

Coulthard, T.J., Kirkby, M.J., Macklin, M.G., 2000. Modelling geomorphic response to environmental change in an upland catchment. Hydrological Processes 14, 2031–2045.

Coulthard, T.J., Macklin, M.G., Kirkby, M.J., 2002. A cellular model of Holocene upland river basin and alluvial fan evolution. Earth Surface Processes and Landforms 27, 269–288.

Coulthard, T.J., Lewin, J., Macklin, M.G., 2005. Modelling differential catchment response to environmental change. Geomorphology 69, 222–241.

Coulthard, T.J., Hicks, M.D., Van De Wiel, M.J., 2007. Cellular modelling of river catchments and reaches: advantages, limitations and prospects. Geomorphology 90, 192–207 (this issue).

Gomez, B., Church, M.A., 1989. An assessment of bedload sediment transport formulae for gravel-bed rivers. Water Resources Research 25, 1161–1186.

Hesselink, A.W., Stelling, G.S., Kwadijk, J.C.J., Middelkoop, H., 2003. Inundation of a Dutch river polder, sensitivity analysis of a physically based inundation model using historic data. Water Resources Research 39, 1234. doi:10.1029/WR2002001334.

Ikeda, S., Parker, G., Sawai, K., 1981. Bend theory of river meanders: I. Linear development. Journal of Fluid Mechanics 112, 363–377.

Johanneson, H., Parker, G., 1989. A linear theory of meanders. In: Ikeda, S., Parker, G. (Eds.), River Meandering. Water Resources Monograph. American Geophysical Union, Washington, D.C., pp. 181–213.

Lane, S.N., 1998. Hydraulic modelling in hydrology and geomorphology: a review of high resolution approaches. Hydrological Processes 12, 1131–1150.

Lauer, J.W., Parker, G., 2005. Net transfer of sediment from floodplain to channel on three southern U.S. rivers. Proceedings of the ASCE World Water and Environmental Resources 2005 Congress, Anchorage, Alaska, May 15–19, 2005. doi:10.1061/40792(173)428.

Murray, A.B., 2003. Contrasting the goals, strategies, and predictions associated with simplified numerical models and detailed simulations. In: Wilcock, P.R., Iverson, R.M. (Eds.), Prediction in Geomorphology. Geophysical Monograph. American Geophysical Union, Washington, DC, pp. 151–165.

Murray, A.B., Paola, C., 1994. A cellular model of braided rivers. Nature 371, 54–57.

Nanson, G.C., Hickin, E.J., 1983. Channel migration and incision on the Beatton River. Journal of Hydraulic Engineering 109, 327–337.

Nicholas, A.P., Mitchell, C.A., 2003. Numerical simulation of overbank processes in topographically complex floodplain environments. Hydrological Processes 17, 727–746.

Sun, T., Meakin, P., Jøssang, T., 2001. A computer model for meandering rivers with multiple bedload sediment sizes. 1. Theory. Water Resources Research 37, 2227–2241.

Thomas, R., Nicholas, A.P., 2002. Simulation of braided flow using a new cellular routing scheme. Geomorphology 43, 179–195.

US Army Corps of Engineers, 2003. HEC-RAS River Analysis System: User's Manual. USACE Hydrologic Engineering Center.

Werner, B.T., 2003. Modeling landforms as self-organized, hierarchical dynamical systems. In: Wilcock, P.R., Iverson, R.M. (Eds.), Prediction in Geomorphology. Geophysical Monograph. American Geophysical Union, Washington, DC, pp. 133–150.

Wilcock, P.R., Crowe, J.C., 2003. Surface-based transport model for mixed-size sediment. Journal of Hydraulic Engineering, ASCE 129, 120–128.

Willgoose, G., 2005. Mathematical modelling of whole landscape evolution. Annual Review of Earth and Planetary Science 33, 433–459.